Study of $h_c \to 3(\pi^+\pi^-)\pi^0$, $h_c \to 2(\pi^+\pi^-)\omega$, $h_c \to 2(\pi^+\pi^-)\pi^0\eta$, $h_c \to 2(\pi^+\pi^-)\eta$, and $h_c \to p\bar{p}$

M. Ablikim *et al.*[*]
(BESIII Collaboration)

(Received 6 March 2024; accepted 4 April 2024; published 30 April 2024)

Based on $(2712.4 \pm 14.1) \times 10^6$ $\psi(3686)$ events collected with the BESIII detector, we study the decays $h_c \to 3(\pi^+\pi^-)\pi^0$, $h_c \to 2(\pi^+\pi^-)\omega$, $h_c \to 2(\pi^+\pi^-)\pi^0\eta$, $h_c \to 2(\pi^+\pi^-)\eta$, and $h_c \to p\bar{p}$ via $\psi(3686) \to \pi^0 h_c$. The decay channel $h_c \to 3(\pi^+\pi^-)\pi^0$ is observed for the first time, and its branching fraction is determined to be $(9.28 \pm 1.14 \pm 0.77) \times 10^{-3}$, where the first uncertainty is statistical and the second is systematic. In addition, first evidence is found for the modes $h_c \to 2(\pi^+\pi^-)\pi^0\eta$ and $h_c \to 2(\pi^+\pi^-)\omega$ with significances of 4.8σ and 4.7σ, and their branching fractions are determined to be $(7.55 \pm 1.51 \pm 0.77) \times 10^{-3}$ and $(4.00 \pm 0.86 \pm 0.35) \times 10^{-3}$, respectively. No significant signals of $h_c \to 2(\pi^+\pi^-)\eta$ and $h_c \to p\bar{p}$ are observed, and the upper limits of the branching fractions of these decays are determined to be $<6.19 \times 10^{-4}$ and $<4.40 \times 10^{-5}$ at the 90% confidence level, respectively.

DOI: 10.1103/PhysRevD.109.072018

I. INTRODUCTION

Studies of charmonium decays play an important role in understanding the structure of quantum chromodynamics (QCD). Despite the success of QCD in describing many aspects of the strong interaction, some applications in charmonium decay mechanism remain challenging, and inconsistencies between experimental results and theoretical predictions have been reported [1].

Since the discovery of the spin-singlet charmonium state $h_c(^1P_1)$ in 2005 [2,3], many theoretical and experimental efforts have been made to understand its properties. Kuang predicted the branching fraction (BF) $\mathcal{B}(h_c \to \text{light hadrons})$ to be $(8.8 \pm 0.8)\%$ and $(48 \pm 7)\%$ with the perturbative QCD and nonrelativistic QCD models [4], respectively. Godfrey and Rosner made a prediction of $\mathcal{B}(h_c \to ggg) = 57\%$ based on QCD calculations [5]. The significant differences between the results of these calculations arise from the use of different computational methods based on various theoretical models and the consideration of different effects. Recently, BESIII reported the BF of the electric dipole (E1) transition to be $\mathcal{B}(h_c \to \gamma\eta_c) = (57.66^{+3.62}_{-3.50} \pm 0.58)\%$ [6], which is reasonably close to some theoretical predictions [4,5]. This implies that nearly half of h_c decays proceed via non-E1 transition. However, the sum of the BFs of the known h_c non-E1 decays is only about 4% [7,8], indicating that the search for new h_c decay modes is well motivated.

In massless QCD models, the $h_c(^1P_1)$ decay into $p\bar{p}$ is forbidden due to the helicity selection rule [9]. However, the observation of the decays $\eta_c/\chi_{c0} \to p\bar{p}$ [7] and the observation of h_c formation in the $p\bar{p}$ annihilation [10] indicate substantial contributions from the effects of finite masses. These observations have stimulated theoretical calculations for the decay $h_c \to p\bar{p}$, arising from which a large BF of the order of 10^{-3} is suggested [11,12]. However, searches until now have not observed a significant signal [13]. Further experimental study of this decay is highly desirable to better understand the underlying dynamical mechanism in $h_c \to p\bar{p}$ decay.

In this paper, we report searches for the undiscovered decay channels of $h_c \to 3(\pi^+\pi^-)\pi^0$, $h_c \to 2(\pi^+\pi^-)\omega$, $h_c \to 2(\pi^+\pi^-)\pi^0\eta$, $h_c \to 2(\pi^+\pi^-)\eta$, and $h_c \to p\bar{p}$ via $\psi(3686) \to \pi^0 h_c$, performed through the analysis of $(2712.4 \pm 14.1) \times 10^6$ $\psi(3686)$ events [14] collected with the BESIII detector in 2009, 2012, and 2021.

II. BESIII DETECTOR AND MONTE CARLO SIMULATION

The BESIII detector [15] records e^+e^- collisions provided by the BEPCII storage ring [16] in the center-of-mass energy range from 2.0 to 4.95 GeV, with a peak luminosity of 1×10^{33} cm^{-2} s^{-1} achieved at $\sqrt{s} = 3.77$ GeV. BESIII has collected large data samples in this energy region [17–19]. The cylindrical core of the BESIII detector covers 93% of the full solid angle and consists of a helium-based multilayer drift chamber (MDC), a plastic scintillator

[*]Full author list given at the end of the article.

time-of-flight system (TOF), and a CsI(Tl) electromagnetic calorimeter (EMC), which are all enclosed in a superconducting solenoidal magnet providing a 1.0 T magnetic field (0.9 T in 2012). The magnet is supported by an octagonal flux-return yoke with modules of resistive plate muon counters interleaved with steel. The charged-particle momentum resolution at 1 GeV/c is 0.5%, and the dE/dx resolution is 6% for the electrons from Bhabha scattering. The EMC measures photon energy with a resolution of 2.5% (5%) at 1 GeV in the barrel (end-cap) region. The time resolution of the TOF barrel part is 68 ps, while that of the end-cap part is 110 ps. The end-cap TOF system was upgraded in 2015 using multigap resistive plate chamber technology, providing a time resolution of 60 ps, which benefits ~83% of the data used in this analysis [20–22].

Monte Carlo (MC) simulated data samples produced with a Geant4-based [23] software package, which includes the geometric description [24] of the BESIII detector and the detector response, are used to optimize the event selection criteria, to estimate the signal efficiency and the level of background. The simulation models the beam-energy spread and initial-state radiation in the e^+e^- annihilation using the generator KKMC [25,26]. The inclusive MC sample includes the production of the $\psi(3686)$ resonance, the initial-state radiation production of the J/ψ meson, and the continuum processes incorporated in KKMC. Particle decays are generated by Evtgen [27,28] for the known decay modes with BFs taken from the Particle Data Group (PDG) [7] and LUNDCHARM [29,30] for the unknown ones. Final-state radiation from charged final-state particles is included using the PHOTOS package [31].

For the exclusive MC simulation samples, the five channels of interest are generated using a phase-space (PHSP) model for each signal mode.

III. EVENT SELECTION

Charged tracks reconstructed in the MDC are required to originate from a region within 10 cm from the nominal interaction point along the symmetry axis of the MDC (z axis) and within 1 cm in the perpendicular plane. The track polar angle θ measured with respect to the z axis must be within the fiducial volume of the MDC, $|\cos\theta| < 0.93$. The tracks are assumed to be protons for $h_c \to p\bar{p}$ decay and pions for other decay modes. Finally, a vertex fit constraining all charged particles to originate from a common vertex is performed.

Photon candidates are reconstructed from isolated electromagnetic showers produced in the crystals of the EMC. The deposited energy of each shower must be greater than 25 MeV in the barrel region ($|\cos\theta| < 0.80$) or greater than 50 MeV in the end-cap region ($0.86 < |\cos\theta| < 0.92$). To suppress electronic noise and energy depositions not associated with the event, the EMC cluster timing is required to be within 700 ns of the start time of the reconstructed event. To form a π^0 candidate, the invariant mass of the selected $\gamma\gamma$ pair is constrained to the known π^0 mass [7] by a one-constraint (1C) kinematic fit, and the $\chi^2_{\rm 1C}$ is required to be less than 20. To form an η candidate, the invariant mass of the selected $\gamma\gamma$ pair is constrained to the known η mass [7] with the loosest $\chi^2_{\rm 1C}$ requirement.

To further suppress background, a $(4+\mathrm{N})$C kinematic fit is performed, which constrains the 4-momentum of the final state to that of the initial system, while the masses of all π^0 and η candidates (denoted by N) are constrained to their nominal masses. The kinematics of the final state tracks are updated through the above kinematic fit. A requirement is placed on the $\chi^2_{(4+\mathrm{N})\mathrm{C}}$ value of the $(4+\mathrm{N})$C fit depending on the final state (see Table I). The value of the requirement is determined by maximizing the figure of merit, defined as $S/\sqrt{S+B}$. Here, S and B are the expected numbers of signal and background events, respectively, obtained from the MC simulation. If there is any excess of photon candidates in an event, then all combinations are considered, and the one with the smallest $\chi^2_{(4+\mathrm{N})\mathrm{C}}$ is kept.

To suppress contamination from decays with unexpected numbers of photons, such as $\psi(3686) \to \gamma\chi_{c2}$ with χ_{c2} decaying to the same final states as the h_c, we require $\chi^2_{4\mathrm{C},n\gamma} < \chi^2_{4\mathrm{C},(n-1)\gamma}$ for $h_c \to 3(\pi^+\pi^-)\pi^0$, $h_c \to 2(\pi^+\pi^-)\omega$, and $h_c \to 2(\pi^+\pi^-)\pi^0\eta$. Here, $\chi_{4\mathrm{C},n\gamma}$ is obtained from a 4C kinematic fit including n photons expected for the signal candidate, while $\chi^2_{4\mathrm{C},(n-1)\gamma}$ is determined from an additional 4C fit with one missing photon compared to the signal decay, respectively. Similarly, in the $h_c \to 2(\pi^+\pi^-)\pi^0\eta$ mode, the background of $\psi(3686) \to 2(\pi^+\pi^-)3\pi^0$ is suppressed by requiring $\chi^2_{7\mathrm{C}}(2\pi^0\eta 2(\pi^+\pi^-)) < \chi^2_{7\mathrm{C}}(3\pi^0 2(\pi^+\pi^-))$.

TABLE I. Requirements on $\chi^2_{(4+\mathrm{N})\mathrm{C}}$, mass windows, and the polar angle of the proton or antiproton ($\cos\theta_{p(\bar{p})}$) for different signal decays. M and m denote the measured invariant mass and the known mass [7] of the indicated particle, respectively.

Mode	$\chi^2_{(4+\mathrm{N})\mathrm{C}}$	Veto
$3(\pi^+\pi^-)\pi^0$	<35	$\lvert RM(\pi^+\pi^-) - m_{J/\psi}\rvert > 12$ (MeV/c^2)
		$\lvert RM(\pi^0\pi^0) - m_{J/\psi}\rvert > 30$ (MeV/c^2)
		$\lvert M(\pi^+\pi^-\pi^0_L) - m_\eta\rvert > 17$ (MeV/c^2)
$2(\pi^+\pi^-)\pi^0\eta$	<20	$\lvert RM(\pi^+\pi^-) - m_{J/\psi}\rvert > 8$ (MeV/c^2)
		$\lvert RM(\pi^0\pi^0) - m_{J/\psi}\rvert > 18$ (MeV/c^2)
		$\lvert RM(\eta) - m_{J/\psi}\rvert > 7$ (MeV/c^2)
		$\lvert M(\pi^+\pi^-\pi^0_L) - m_\eta\rvert > 12$ (MeV/c^2)
		$\lvert M(\pi^+\pi^-\pi^0_L) - m_\omega\rvert > 26$ (MeV/c^2)
$2(\pi^+\pi^-)\eta$	<25	$\lvert RM(\pi^+\pi^-) - m_{J/\psi}\rvert > 15$ (MeV/c^2)
		$\lvert RM(\eta) - m_{J/\psi}\rvert > 10$ (MeV/c^2)
		$\lvert M(\pi^+\pi^-\pi^0_L) - m_\eta\rvert > 15$ (MeV/c^2)
		$\lvert M(\pi^+\pi^-\pi^0_L) - m_\omega\rvert > 26$ (MeV/c^2)
$p\bar{p}$	<15	$\lvert\cos\theta_{p(\bar{p})}\rvert < 0.8$

The J/ψ-related background is vetoed by the requirements on the $\pi^0\pi^0$, $\pi^+\pi^-$, and η recoil-mass windows. The mass windows are listed in Table I, where RM denotes the recoiling mass, defined as $RM(X) = \sqrt{(p_{\psi(3686)} - p_X)^2}$, where $p_{\psi(3686)}$ and p_X are the four momenta of $\psi(3686)$ and X, respectively. Here, the $\psi(3686) \to \pi^+\pi^- J/\psi$ candidates are selected by minimizing $|RM(\pi^+\pi^-) - m_{J/\psi}|$ in the multiple $\pi^+\pi^-$ combinations, which will introduce the potential wrong combination background. Subsequently, the mass window used to veto J/ψ-related background by $\pi^+\pi^-$ recoil mass is flexible, depending on the wrong combination background level. For the $h_c \to p\bar{p}$ reconstruction, the background from lepton pairs originating from J/ψ decays is suppressed by requiring $|\cos\theta_{p(\bar{p})}| < 0.8$, where $\theta_{p(\bar{p})}$ is the polar angle of the proton (antiproton) candidate. The energy of the π^0 from the h_c decay is typically larger than the energy of the bachelor π^0 from $\psi(3686) \to \pi^0 h_c$. In events with two neutral pions, the one with smaller energy is denoted π^0_L while the other is denoted π^0_H. The bachelor π^0_L should not form any resonance in combination with other final-state particles. Therefore, additional vetoes, summarized in Table I, are applied to suppress background from $\eta, \omega \to \pi^+\pi^-\pi^0_L$.

In the case of candidate $h_c \to 3(\pi^+\pi^-)\pi^0$ decays, we examine the invariant-mass spectrum of $\pi^+\pi^-\pi^0_H$ to check for the presence of an ω intermediate state. The ω signal region for $h_c \to 2(\pi^+\pi^-)\omega$ is set to be $|M(\pi^+\pi^-\pi^0_H) - m_\omega| < 20$ MeV/c^2, and the ω sideband region is set to be $60 < |M(\pi^+\pi^-\pi^0_H) - m_\omega| < 100$ MeV/c^2, where m_ω is the known ω mass [7], as shown in Fig. 1. All mass windows are determined to account for the respective mass resolutions.

The invariant-mass distributions for the four h_c decay modes and the intermediate process $h_c \to 2(\pi^+\pi^-)\omega$, after all selection criteria, are shown in Fig. 2. The potential backgrounds are investigated with the inclusive $\psi(3686)$ MC events, using the event-type analysis tool TopoAna [32]. It is found that for the $h_c \to 2(\pi^+\pi^-)\pi^0\eta$ selection there are peaking background contributions from $\psi(3686) \to \pi^0 h_c$, $h_c \to \gamma\eta_c$, $\eta_c \to 2(\pi^+\pi^-)\eta$, or $\eta_c \to 2(\pi^+\pi^-\pi^0)$, and for the $h_c \to 2(\pi^+\pi^-)\eta$ selection there are peaking background contributions from $h_c \to \gamma\eta_c$, $\eta_c \to \pi^+\pi^-\eta'$, $\eta' \to \pi^+\pi^-\gamma$, or $\eta_c \to 2(\pi^+\pi^-)\pi^0$. Misidentification of photons as π^0/η in these background processes can contaminate the signal region. The size of these background contributions is estimated through MC studies and included in the fit. The BF of the decay $\eta_c \to 2(\pi^+\pi^-)\pi^0$ is currently unknown, which is reflected in the assignment of the systematic uncertainties. Additionally, the BFs for the other mentioned background processes are taken from the PDG [7].

To investigate contamination from continuum background, the same selection criteria are applied to the data samples collected at the center-of-mass energy of 3.65 GeV, corresponding to an integrated luminosity of 454 pb^{-1}. No h_c candidates are found. Therefore, continuum background is considered to be at a negligible level.

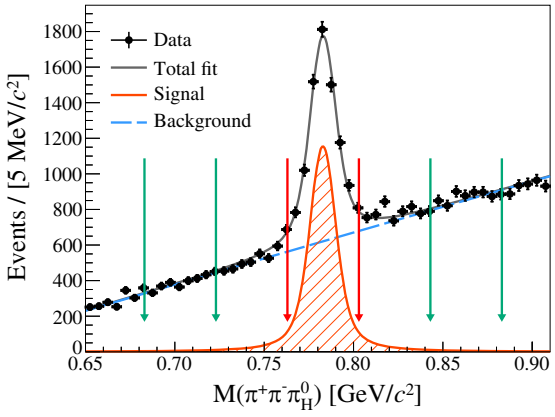

FIG. 1. The $M_{\pi^+\pi^-\pi^0_H}$ distribution of the accepted candidates in data. The dotted error bars represent the distribution of different $\pi^+\pi^-\pi^0_H$ combinations overlaid. The pair of red arrows show the ω signal region, and the pair of green arrows show the ω sideband region.

IV. SIGNAL YIELDS

The number of h_c signal events $N^{\rm obs}_{h_c}$ for each signal decay mode is determined from maximum likelihood fits to the corresponding mass spectra, as shown in Fig. 2. For the channels where a signal is observed, the signal shape is described by a convolution of the MC-simulated shape and a Gaussian function accounting for the difference in mass resolution between data and MC simulation, where the width of the Gaussian function is a free parameter in the fit. For the channels with no significant signals observed [$h_c \to 2(\pi^+\pi^-)\eta$ and $h_c \to p\bar{p}$], only the MC-simulated shapes are used. In the fit to the $h_c \to 2(\pi^+\pi^-)\pi^0\eta$ decay, two additional normalized peaking background components from $h_c \to \gamma\eta_c$, $\eta_c \to 2(\pi^+\pi^-)\eta$, and $h_c \to \gamma\eta_c$, $\eta_c \to 2(\pi^+\pi^-\pi^0)$ are included with fixed background contributions of 3.9 and 35.4 events, respectively. Additionally, for the $h_c \to 2(\pi^+\pi^-)\eta$ mode, a contribution of 20 events is included from $h_c \to \gamma\eta_c$, $\eta_c \to \pi^+\pi^-\eta'$ background. The remaining nonpeaking background shape is described by an ARGUS function [33], with end point fixed at the kinematic threshold of 3.551 GeV/c^2. The statistical significance of the $h_c \to 3(\pi^+\pi^-)\pi^0$ decay is greater than 5σ, and that of the intermediate process $h_c \to 2(\pi^+\pi^-)\omega$ in the $3(\pi^+\pi^-)\pi^0$ final state is 4.7σ. The significance for the $h_c \to 2(\pi^+\pi^-)\pi^0\eta$ mode is determined to be 4.8σ. For each signal decay mode, the significance is estimated from the likelihood difference with and without the signal component included in the fit, taking into account the change in the number of degrees of freedom. The systematic uncertainties are considered in determining the final signal significance.

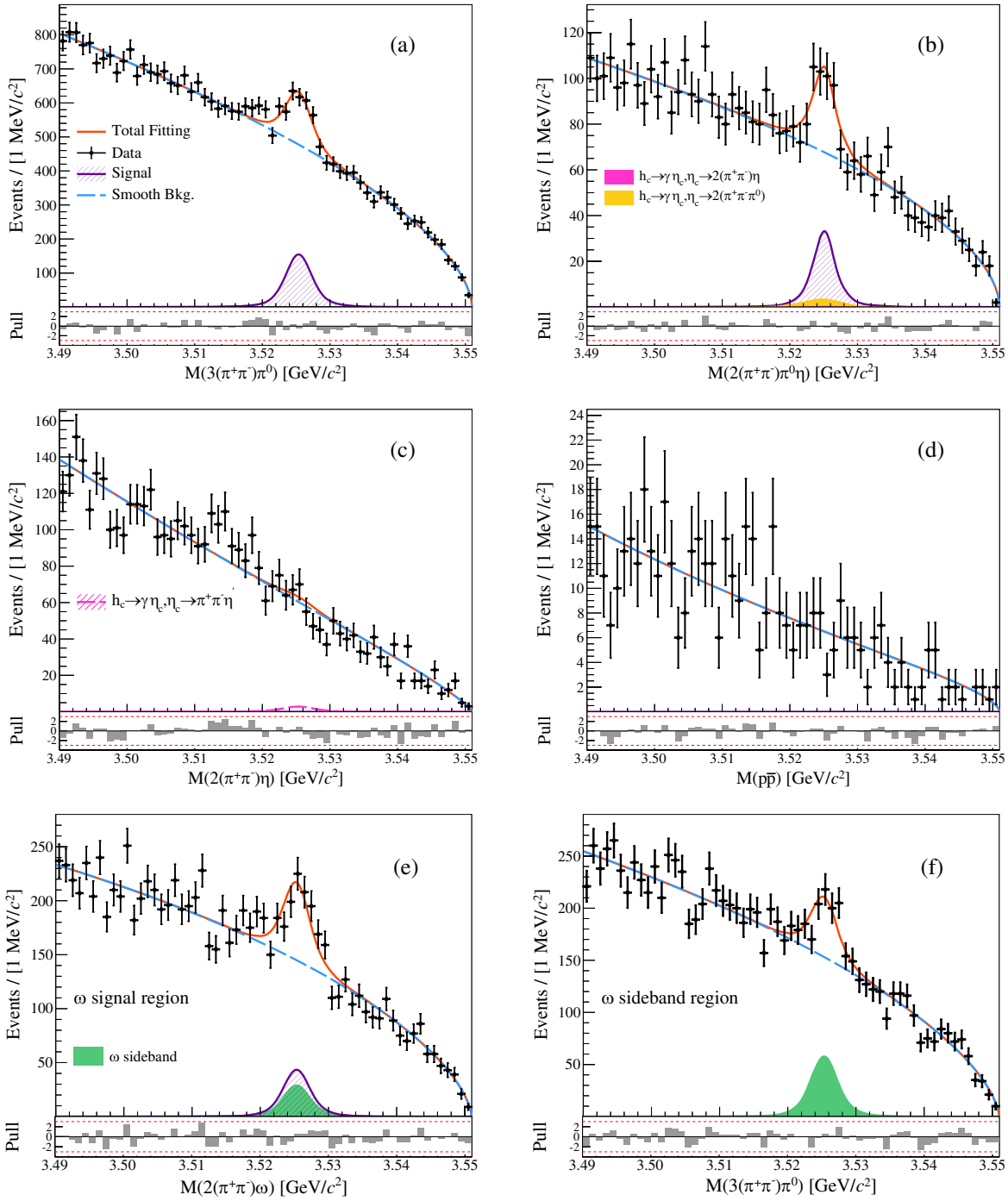

FIG. 2. Fits to the invariant-mass distributions of (a) $h_c \to 3(\pi^+\pi^-)\pi^0$, (b) $h_c \to 2(\pi^+\pi^-)\pi^0\eta$, (c) $h_c \to 2(\pi^+\pi^-)\eta$, (d) $h_c \to p\bar{p}$, (e) $h_c \to 2(\pi^+\pi^-)\omega$ in the ω signal region, and (f) $h_c \to 3(\pi^+\pi^-)\pi^0$ in the ω sideband region. The green histogram shows the scaled h_c peak obtained from the fit to the events inside the ω sideband region. The lower panels of each plot show the fit residuals expressed in number of standard deviations.

The signal yield for $h_c \to 2(\pi^+\pi^-)\omega$ is evaluated by performing a simultaneous fit to the $M(3(\pi^+\pi^-)\pi^0)$ spectra for the events in both ω signal and sideband regions using the signal and background shapes described above. The width of the Gaussian function used for smearing is fixed to the value obtained from the fit for the $h_c \to 3(\pi^+\pi^-)\pi^0$ decay. The h_c yield in the ω sideband region is scaled by a factor $f_\omega = 0.50$, which takes into account the relative difference in the number of events between ω signal and sideband regions, as shown in Fig. 1. Specifically, in the fitting of the $\pi^+\pi^-\pi^0$ invariant mass spectrum, the signal component is modeled with a double Gaussian function.

TABLE II. The number of observed signal events $N^{\rm obs}_{h_c}$, the detection efficiency, the product BF $\mathcal{B}(\psi(3686) \to \pi^0 h_c) \times \mathcal{B}(h_c \to X)$, and the absolute BF $\mathcal{B}(h_c \to X)$. The first and second uncertainties are statistical and systematic, respectively.

			$\mathcal{B}(\psi(3686) \to \pi^0 h_c) \times \mathcal{B}(h_c \to X)$		
Final state (X)	$N^{\rm obs}_{h_c}$	$\epsilon(\%)$	This study	Previous BESIII result	$\mathcal{B}(h_c \to X)$
$3(\pi^+\pi^-)\pi^0$	834.7 ± 102.3	4.64 ± 0.01	$(6.79 \pm 0.83 \pm 0.56) \times 10^{-6}$	$<7.56 \times 10^{-6}$ [7]	$(9.28 \pm 1.14 \pm 0.77) \times 10^{-3}$
$2(\pi^+\pi^-)\pi^0\eta$	154.4 ± 30.8	2.68 ± 0.01	$(5.33 \pm 1.10 \pm 0.56) \times 10^{-6}$	…	$(7.55 \pm 1.51 \pm 0.77) \times 10^{-3}$
$2(\pi^+\pi^-)\eta$	<33.7	7.05 ± 0.01	$<4.53 \times 10^{-7}$	…	$<6.19 \times 10^{-4}$
$p\bar{p}$	12.4	14.35 ± 0.02	$<3.22 \times 10^{-8}$	$<1.3 \times 10^{-7}$ [13]	$<4.40 \times 10^{-5}$
$2(\pi^+\pi^-)\omega$	236.9 ± 50.9	3.42 ± 0.01	$(2.93 \pm 0.63 \pm 0.26) \times 10^{-6}$	…	$(4.00 \pm 0.86 \pm 0.35) \times 10^{-3}$

The remaining combinatorial background shape is described by a first-order polynomial function.

Since no significant signals of $h_c \to 2(\pi^+\pi^-)\eta$ and $h_c \to p\bar{p}$ are observed, the upper limits of the signal yields for these decays are determined to be 33.7 and 12.4, respectively. The upper limit has already incorporated the systematic uncertainty, and the corresponding method is discussed in Sec. V.

The BFs of the h_c decay channels are calculated with

$$\mathcal{B}(h_c \to X) = \frac{N^{\rm obs}_{h_c}}{N_{\psi(3686)} \cdot \mathcal{B}(\psi(3686) \to \pi^0 h_c) \cdot \prod_i \mathcal{B}_i \cdot \varepsilon}. \quad (1)$$

Here, $N^{\rm obs}_{h_c}$ is the number of observed h_c signal events, $N_{\psi(3686)}$ is the total number of $\psi(3686)$ events, X denotes a given final state, $\mathcal{B}_i$ is the BF of the ith intermediate state taken from the PDG [7], and ε is the detection efficiency. The results and related numerical information are given in Table II.

V. SYSTEMATIC UNCERTAINTIES

The sources of systematic uncertainties in the BF measurements are associated with the tracking efficiency, photon-detection efficiency, π^0 or η reconstruction efficiency, kinematic fit, signal-yield extraction, choice of theoretical model, etc. The evaluated contributions to the systematic uncertainties are listed in Table III and discussed below.

(i) *Tracking efficiency*: The tracking efficiency of charged pions is estimated by studying the control sample of $J/\psi \to \pi^+\pi^-\pi^0$ decays. The MC simulation is reweighted in two-dimensional $(\cos\theta, p_t)$ intervals according to the efficiencies obtained from the control sample, where θ is the polar angle and p_t is the transverse momentum of the charged pion. The observed change in the selection efficiency is assigned as the systematic uncertainty. The systematic uncertainties associated with the tracking efficiencies of protons (antiprotons) are estimated with the control samples $J/\psi \to p\bar{p}\pi^+\pi^-$ decays [35], and both of them are assigned as 1.0% for per proton (antiproton).

(ii) *Photon-detection efficiency*: The photon-detection efficiency is studied using a control sample of $e^+e^- \to \gamma\mu^+\mu^-$ events. The difference in the photon detection efficiencies between data and MC simulation, 0.5%, is assigned as the systematic uncertainty for each photon.

(iii) *π^0 and η reconstruction efficiency*: Based on a control sample of $e^+e^- \to \omega\pi^0$ events at $\sqrt{s} = 3.773$ GeV, the difference of the π^0 reconstruction efficiencies between data and MC simulation is studied and found to have the following dependence on momentum: $(0.06\text{–}2.41 \cdot p\,[\mathrm{GeV}/c])\%$. The systematic uncertainty associated with this difference is calculated by averaging this function over the π^0 momentum distribution in each signal decay mode. The uncertainty due to the choice of η mass window is determined to be 1.0% per η, from studies of a high purity control sample of $J/\psi \to p\bar{p}\eta$ decays [36].

(iv) *Kinematic fit*: The systematic uncertainty associated with the kinematic fit is estimated by comparing the efficiencies with and without a helix parameter correction applied to the signal MC events [37]. The assigned systematic uncertainties are (2.1–3.2)% for the different signal decay modes.

(v) *Signal-yield extraction*:

Mass window: To evaluate the systematic uncertainty associated with the choice of mass window, we perform a Barlow test [38] to examine the deviation in significance (ζ) between the baseline fit and that performed for the systematic test. The deviation in significance is defined as

$$\zeta = \frac{|V_{\rm nominal} - V_{\rm test}|}{\sqrt{|\sigma^2_{V\rm nominal} - \sigma^2_{V\rm test}|}}, \quad (2)$$

where V represents the BF; σ_V is the statistical uncertainty on V. For each signal decay, the mass window is varied by up to one times the corresponding mass resolution, with a step of 0.25

times the mass resolution. If the ζ value is not greater than 2, its effect is assumed to be negligible. For the decays where no significant signal is observed, the corresponding systematic uncertainty is assigned as the maximum difference within the various test ranges mentioned earlier (unless otherwise specified, similar situations are estimated using the same method). Additionally, the systematic uncertainty associated with the choice of ω mass window is estimated from a control sample of $\psi(3686) \to K^+K^-\omega$ decays. The differences in the acceptance efficiencies between data and MC simulation are taken as the corresponding systematic uncertainties.

Fit range: The systematic uncertainty arising from the choice of fit range is similarly investigated using the Barlow test. To determine the corresponding ζ distribution, we systematically adjust the fit range by shrinking the interval $(3480, 3551)$ MeV/c^2 to $(3500, 3551)$ MeV/c^2, with a step size of 2 MeV/c^2.

Signal shape: To estimate the systematic uncertainty associated with the choice of signal shape, we use an alternative MC-simulated shape convolved with a double Gaussian function. The difference relative to the nominal fit is taken as the systematic uncertainty.

Background shape: The uncertainties due to the choice of background shape is estimated by replacing the ARGUS function with a second-order Chebychev polynomial function. The change in the fitted signal yield is taken as the systematic uncertainty.

η_c peaking background: The uncertainty associated with the knowledge of the η_c peaking background is estimated according to the uncertainty of the corresponding BF measurements [7,39] or by including this contribution in the fit, assuming $\mathcal{B}(\eta_c \to 2(\pi^+\pi^-)\pi^0)$ is equal to $\mathcal{B}(\eta_c \to 2(\pi^+\pi^-)\eta)$, and assigning the largest differences between these and the baseline results as the systematic uncertainty.

Wrong-combination background: The uncertainty due to the wrong-combination background (WCB) in the π^0 reconstruction is investigated by studying the matching angle between generated and reconstructed momenta. Events containing candidates with matching angles greater than 10° are classified as the WCB background. The possible bias due to WCB is estimated by comparing the signal yields with and without including the WCB contribution in the fits. The difference in the fitted signal yield is taken as the systematic uncertainty.

Normalization factor: The systematic uncertainty related to the normalization factor in calculating the non-ω contribution in extracting the number of the $h_c \to 2(\pi^+\pi^-)\omega$ signal events is estimated by producing multidimensional Gaussian random numbers with the covariance matrix from the fit as input. A group of normalization factors is obtained from this procedure, and the standard deviation of the corresponding distribution is taken as the systematic uncertainty.

ω sideband: The systematic uncertainty due to the choice of ω sideband region is determined by widening and narrowing the range by one standard deviation of the ω mass resolution. The largest change relative to the fitted signal yield for $h_c \to 2(\pi^+\pi^-)\omega$ is taken as the corresponding systematic uncertainty.

(vi) *Theoretical model*: There is a potential systematic bias associated with the choice of theoretical model for the primary decay of $\psi(3686) \to \pi^0 h_c$ and the sequential decay $h_c \to$ hadrons, since these decays are not understood well at present. The difference in reconstruction efficiencies between simulated events generated with the PHSP model and the model proposed in Refs. [27,28] is assigned as the systematic uncertainty for $\psi(3686) \to \pi^0 h_c$. The difference in efficiencies between events generated with the PHSP model and the mixed model including additional intermediate states is taken as the systematic uncertainty for $h_c \to$ hadrons.

(vii) *MC sample size*: The statistical uncertainty in the reconstruction efficiency associated with the finite MC sample size can be calculated as $\Delta_\epsilon = \sqrt{\epsilon(1-\epsilon)/N}$, where ϵ is the reconstruction efficiency, and N is the total number of generated events. The relative uncertainty from this source is Δ_ϵ/ϵ.

(viii) *Input BFs*: The uncertainties in the knowledge of the BFs of $\mathcal{B}(\psi(3686) \to \pi^0 h_c)$, $\mathcal{B}(\eta \to \gamma\gamma)$, and $\mathcal{B}(\omega \to \pi^+\pi^-\pi^0)$, which are 5.6% [39], 0.5% [7], and 0.8% [7], respectively, are assigned as individual systematic uncertainties.

(ix) $N_{\psi(3686)}$: The total number of $\psi(3686)$ events in the sample is determined from inclusive hadronic $\psi(3686)$ decays with an uncertainty of 0.5% [14].

The systematic uncertainties are summarized in Table III. For each signal decay mode, the total systematic uncertainty is obtained by adding all contributions in quadrature under the assumption that they are independent.

The systematic uncertainty from the upper limit of signal events $N^{\rm obs}_{h_c}$ at 90% confidence level includes additive sources and multiplicative sources. To account for the additive systematic uncertainties related to the fits, several alternative fits are performed. These alternative fits involve signal shape, background shape, η_c peaking-background shape as well as different fit ranges, and the one resulting the most conservative upper limit is chosen. Then, the

TABLE III. Relative systematic uncertainties (in percent) for each h_c decay channel. The dash indicates that the systematic uncertainty is not applicable. Asterisk denotes that the additive systematic uncertainty values are invalid.

Source	$3(\pi^+\pi^-)\pi^0$	$2(\pi^+\pi^-)\pi^0\eta$	$2(\pi^+\pi^-)\eta$	$p\bar{p}$	$2(\pi^+\pi^-)\omega$
Tracking	2.3	1.6	1.4	2.0	2.3
Photon efficiency	2.0	3.0	2.0	1.0	2.0
π^0 reconstruction	2.1	2.2	0.5	0.5	1.6
η reconstruction	···	1.0	1.0	···	···
Kinematic fit	2.1	2.3	2.5	3.2	2.3
Mass window	Negligible	1.2	6.8	···	1.1
Signal shape	0.8	0.3	*	*	2.1
Background shape	2.6	4.1	*	*	2.5
η_c peaking-background shape	···	1.8	*	···	···
WCB	1.3	1.9	···	···	Negligible
Fit range	Negligible	Negligible			Negligible
Normalization factor	···	···	···	···	0.5
ω sideband	···	···	···	···	3.8
Theoretical model	3.1	5.0	0.1	Negligible	0.6
MC sample size	0.2	0.1	0.1	0.3	0.4
Input BFs	5.6	5.6	5.6	5.6	5.7
$N_{\psi(3686)}$	0.5	0.5	0.5	0.5	0.5
Sum	8.3	10.2	13.7	11.2	8.8

multiplicative systematic uncertainty is incorporated in the calculation of the upper limit via [40,41]

$$L'(N) = \int_0^1 L\left(\frac{S}{\hat{S}}N\right)\exp\left[-\frac{(S-\hat{S})}{2\sigma_S^2}\right]dS, \qquad (3)$$

where, $L(N)$ is the likelihood distribution as a function of signal events, N; S is the expected efficiency, and $\hat{S}$ is the nominal efficiency; σ_S is its multiplicative systematic uncertainty coming from Table III. Following these steps, the corresponding likelihood distribution can be obtained as shown in Fig. 3. The assumed yields for processes $h_c \to 2(\pi^+\pi^-)\eta$ and $h_c \to p\bar{p}$ at 90% confidence level are set as upper limits, and the corresponding BF calculated using Eq. (1) is the upper limit BF, as shown in Table II.

VI. SUMMARY

By analyzing $(2712.4 \pm 14.1) \times 10^6$ $\psi(3686)$ events collected in the BESIII experiment, we report the observation of $h_c \to 3(\pi^+\pi^-)\pi^0$, as well as evidence for the decays $h_c \to 2(\pi^+\pi^-)\pi^0\eta$ and $h_c \to 2(\pi^+\pi^-)\omega$. We have also searched for $h_c \to 2(\pi^+\pi^-)\eta$ and $h_c \to p\bar{p}$, but no significant signal is observed for both decays. The measured BFs or upper limits at the 90% confidence level are listed in Table II. The upper limit on $\mathcal{B}(h_c \to p\bar{p})$ is a factor of three lower than that set in previous studies [13]. Furthermore, the limit is a factor of 100 lower than the predictions found in Refs. [11,12], which indicates the need for improved theoretical calculations as well as more sensitive measurements.

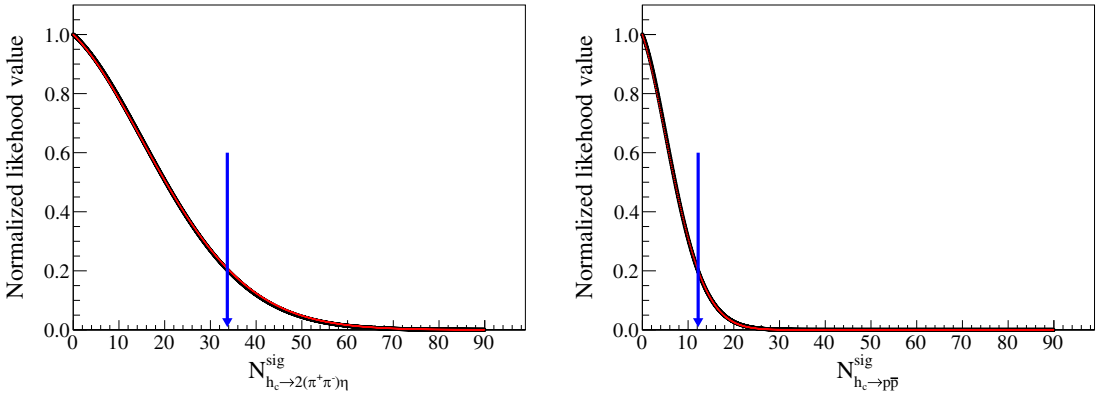

FIG. 3. The normalized likelihood distribution for (left) $h_c \to 2(\pi^+\pi^-)\eta$ and (right) $h_c \to p\bar{p}$ mode. The results obtained with and without incorporating the systematic uncertainties are shown in blue dots and black dots, respectively. The arrow is the position of the upper limit on the signal yields at 90% confidence level.

ACKNOWLEDGMENTS

The BESIII Collaboration thanks the staff of BEPCII and the IHEP computing center for their strong support. This work is supported in part by National Key R&D Program of China under Contracts No. 2020YFA0406300 and No. 2020YFA0406400; National Natural Science Foundation of China (NSFC) under Contracts No. 11635010, No. 11735014, No. 11835012, No. 11935015, No. 11935016, No. 11935018, No. 11961141012, No. 12022510, No. 12025502, No. 12035009, No. 12035013, No. 12061131003, No. 12192260, No. 12192261, No. 12192262, No. 12192263, No. 12192264, No. 12192265, No. 12221005, No. 12225509, No, 12235017, and No. 12150004; Program of Science and Technology Development Plan of Jilin Province of China under Contracts No. 20210508047RQ and No. 20230101021JC; the Chinese Academy of Sciences (CAS) Large-Scale Scientific Facility Program; the CAS Center for Excellence in Particle Physics (CCEPP); Joint Large-Scale Scientific Facility Funds of the NSFC and CAS under Contract No. U1832207; CAS Key Research Program of Frontier Sciences under Contracts No. QYZDJ-SSW-SLH003 and No. QYZDJ-SSW-SLH040; 100 Talents Program of CAS; The Institute of Nuclear and Particle Physics (INPAC) and Shanghai Key Laboratory for Particle Physics and Cosmology; European Union's Horizon 2020 research and innovation programme under Marie Sklodowska-Curie grant agreement under Contract No. 894790; German Research Foundation DFG under Contracts No. 455635585, Collaborative Research Center CRC 1044, FOR5327, and GRK 2149; Istituto Nazionale di Fisica Nucleare, Italy; Ministry of Development of Turkey under Contract No. DPT2006K-120470; National Research Foundation of Korea under Contract No. NRF-2022R1A2C1092335; National Science and Technology fund of Mongolia; National Science Research and Innovation Fund (NSRF) via the Program Management Unit for Human Resources & Institutional Development, Research and Innovation of Thailand under Contract No. B16F640076; Polish National Science Centre under Contract No. 2019/35/O/ST2/02907; The Swedish Research Council; and U.S. Department of Energy under Contract No. DE-FG02-05ER41374.

[1] E. Eichten, S. Godfrey, H. Mahlke, and J. L. Rosner, Rev. Mod. Phys. **80**, 1161 (2008).
[2] P. Rubin *et al.* (CLEO Collaboration), Phys. Rev. D **72**, 092004 (2005).
[3] J. L. Rosner *et al.* (CLEO Collaboration), Phys. Rev. Lett. **95**, 102003 (2005).
[4] Y.-P. Kuang, Phys. Rev. D **65**, 094024 (2002).
[5] S. Godfrey and J. L. Rosner, Phys. Rev. D **66**, 014012 (2002).
[6] M. Ablikim *et al.* (BESIII Collaboration), Phys. Rev. D **106**, 072007 (2022).
[7] P. L. Workman *et al.* (Particle Data Group), Prog. Theor. Exp. Phys. **2022**, 083C01 (2022).
[8] M. Ablikim *et al.* (BESIII Collaboration), J. High Energy Phys. 05 (2022) 108.
[9] S. J. Brodsky and G. P. Lepage, Phys. Rev. D **24**, 2848 (1981).
[10] M. Andreotti *et al.* (Fermilab E835 Collaboration), Phys. Rev. D **72**, 032001 (2005).
[11] X. H. Liu and Q. Zhao, J. Phys. G **38**, 035007 (2011).
[12] S. Barsuk, J. He, E. Kou, and B. Viaud, Phys. Rev. D **86**, 034011 (2012).
[13] M. Ablikim *et al.* (BESIII Collaboration), Phys. Rev. D **88**, 112001 (2013).
[14] M. Ablikim *et al.* (BESIII Collaboration), arXiv:2403.06766.
[15] M. Ablikim *et al.* (BESIII Collaboration), Nucl. Instrum. Methods Phys. Res., Sect. A **614**, 345 (2010).
[16] C. H. Yu *et al.*, *Proceedings of IPAC2016, Busan, Korea* (JACoW, Busan, 2016), https://accelconf.web.cern.ch/ipac2016/.
[17] M. Ablikim *et al.* (BESIII Collaboration), Chin. Phys. C **44**, 040001 (2020).
[18] J. Lu, Y. Xiao, and X. Ji, Radiat. Detect. Technol. Methods **4**, 337 (2020).
[19] J. W. Zhang, L. H. Wu, S. S. Sun *et al.*, Radiat. Detect. Technol. Methods **6**, 289 (2022).
[20] X. Li *et al.*, Radiat. Detect. Technol. Methods **1**, 13 (2017).
[21] Y. X. Guo *et al.*, Radiat. Detect. Technol. Methods **1**, 15 (2017).
[22] P. Cao *et al.*, Nucl. Instrum. Methods Phys. Res., Sect. A **953**, 163053 (2020).
[23] S. Agostinelli *et al.* (GEANT4 Collaboration), Nucl. Instrum. Methods Phys. Res., Sect. A **506**, 250 (2003).
[24] K. X. Huang *et al.*, Nucl. Sci. Tech. **33**, 142 (2022).
[25] S. Jadach, B. F. L. Ward, and Z. Was, Comput. Phys. Commun. **130**, 260 (2000).
[26] S. Jadach, B. F. L. Ward, and Z. Was, Phys. Rev. D **63**, 113009 (2001).
[27] R. G. Ping, Chin. Phys. C **32**, 599 (2008).
[28] D. J. Lange, Nucl. Instrum. Methods Phys. Res., Sect. A **462**, 152 (2001).
[29] J. C. Chen, G. S. Huang, X. R. Qi, D. H. Zhang, and Y. S. Zhu, Phys. Rev. D **62**, 034003 (2000).
[30] R. L. Yang, R. G. Ping, and H. Chen, Chin. Phys. Lett. **31**, 061301 (2014).

[31] E. Richter-Was, Phys. Lett. B **303**, 163 (1993).
[32] X. Y. Zhou, S. X. Du, G. Li, and C. P. Shen, Comput. Phys. Commun. **258**, 107540 (2021).
[33] H. Albrecht *et al.*, Phys. Lett. B **340**, 217 (1994).
[34] Gary J. Feldman and Robert D. Cousins, Phys. Rev. D **57**, 3873 (1998).
[35] W. L. Yuan, X.-C. Ai, X.-B. Ji, S.-J. Chen, Y. Zhang, L.-H. Wu, L.-L. Wang, and Y. Yuan, Chin. Phys. C **40**, 026201 (2016).
[36] M. Ablikim *et al.* (BESIII Collaboration), Phys. Rev. D **81**, 052005 (2010).
[37] M. Ablikim *et al.* (BESIII Collaboration), Phys. Rev. D **87**, 012002 (2013).
[38] O. Behnke, K. Kroninger, G. Schott, and T. H. Schorner-Sadenius, *Data Analysis in High Energy Physics: A Practical Guide to Statistical Methods* (Wiley-VCH, Berlin, Germany, 2013).
[39] M. Ablikim *et al.* (BESIII Collaboration), Phys. Rev. D **106**, 072007 (2022).
[40] K. Stenson, arXiv:physics/0605236.
[41] X. X. Liu, X. R. Lyu, and Y. S. Zhu, Chin. Phys. C **39**, 113001 (2015).

M. Ablikim,[1] M. N. Achasov,[4,c] P. Adlarson,[75] O. Afedulidis,[3] X. C. Ai,[80] R. Aliberti,[35] A. Amoroso,[74a,74c] Q. An,[71,58,a] Y. Bai,[57] O. Bakina,[36] I. Balossino,[29a] Y. Ban,[46,h] H.-R. Bao,[63] V. Batozskaya,[1,44] K. Begzsuren,[32] N. Berger,[35] M. Berlowski,[44] M. Bertani,[28a] D. Bettoni,[29a] F. Bianchi,[74a,74c] E. Bianco,[74a,74c] A. Bortone,[74a,74c] I. Boyko,[36] R. A. Briere,[5] A. Brueggemann,[68] H. Cai,[76] X. Cai,[1,58] A. Calcaterra,[28a] G. F. Cao,[1,63] N. Cao,[1,63] S. A. Cetin,[62a] J. F. Chang,[1,58] G. R. Che,[43] G. Chelkov,[36,b] C. Chen,[43] C. H. Chen,[9] Chao Chen,[55] G. Chen,[1] H. S. Chen,[1,63] H. Y. Chen,[20] M. L. Chen,[1,58,63] S. J. Chen,[42] S. L. Chen,[45] S. M. Chen,[61] T. Chen,[1,63] X. R. Chen,[31,63] X. T. Chen,[1,63] Y. B. Chen,[1,58] Y. Q. Chen,[34] Z. J. Chen,[25,i] Z. Y. Chen,[1,63] S. K. Choi,[10] G. Cibinetto,[29a] F. Cossio,[74c] J. J. Cui,[50] H. L. Dai,[1,58] J. P. Dai,[78] A. Dbeyssi,[18] R. E. de Boer,[3] D. Dedovich,[36] C. Q. Deng,[72] Z. Y. Deng,[1] A. Denig,[35] I. Denysenko,[36] M. Destefanis,[74a,74c] F. De Mori,[74a,74c] B. Ding,[66,1] X. X. Ding,[46,h] Y. Ding,[40] Y. Ding,[34] J. Dong,[1,58] L. Y. Dong,[1,63] M. Y. Dong,[1,58,63] X. Dong,[76] M. C. Du,[1] S. X. Du,[80] Y. Y. Duan,[55] Z. H. Duan,[42] P. Egorov,[36,b] Y. H. Fan,[45] J. Fang,[59] J. Fang,[1,58] S. S. Fang,[1,63] W. X. Fang,[1] Y. Fang,[1] Y. Q. Fang,[1,58] R. Farinelli,[29a] L. Fava,[74b,74c] F. Feldbauer,[3] G. Felici,[28a] C. Q. Feng,[71,58] J. H. Feng,[59] Y. T. Feng,[71,58] M. Fritsch,[3] C. D. Fu,[1] J. L. Fu,[63] Y. W. Fu,[1,63] H. Gao,[63] X. B. Gao,[41] Y. N. Gao,[46,h] Yang Gao,[71,58] S. Garbolino,[74c] I. Garzia,[29a,29b] L. Ge,[80] P. T. Ge,[76] Z. W. Ge,[42] C. Geng,[59] E. M. Gersabeck,[67] A. Gilman,[69] K. Goetzen,[13] L. Gong,[40] W. X. Gong,[1,58] W. Gradl,[35] S. Gramigna,[29a,29b] M. Greco,[74a,74c] M. H. Gu,[1,58] Y. T. Gu,[15] C. Y. Guan,[1,63] Z. L. Guan,[22] A. Q. Guo,[31,63] L. B. Guo,[41] M. J. Guo,[50] R. P. Guo,[49] Y. P. Guo,[12,g] A. Guskov,[36,b] J. Gutierrez,[27] K. L. Han,[63] T. T. Han,[1] F. Hanisch,[3] X. Q. Hao,[19] F. A. Harris,[65] K. K. He,[55] K. L. He,[1,63] F. H. Heinsius,[3] C. H. Heinz,[35] Y. K. Heng,[1,58,63] C. Herold,[60] T. Holtmann,[3] P. C. Hong,[34] G. Y. Hou,[1,63] X. T. Hou,[1,63] Y. R. Hou,[63] Z. L. Hou,[1] B. Y. Hu,[59] H. M. Hu,[1,63] J. F. Hu,[56,j] S. L. Hu,[12,g] T. Hu,[1,58,63] Y. Hu,[1] G. S. Huang,[71,58] K. X. Huang,[59] L. Q. Huang,[31,63] X. T. Huang,[50] Y. P. Huang,[1] T. Hussain,[73] F. Hölzken,[3] N. Hüsken,[35] N. Hüsken,[27,35] N. in der Wiesche,[68] J. Jackson,[27] S. Janchiv,[32] J. H. Jeong,[10] Q. Ji,[1] Q. P. Ji,[19] W. Ji,[1,63] X. B. Ji,[1,63] X. L. Ji,[1,58] Y. Y. Ji,[50] X. Q. Jia,[50] Z. K. Jia,[71,58] D. Jiang,[1,63] H. B. Jiang,[76] P. C. Jiang,[46,h] S. S. Jiang,[39] T. J. Jiang,[16] X. S. Jiang,[1,58,63] Y. Jiang,[63] J. B. Jiao,[50] J. K. Jiao,[34] Z. Jiao,[23] S. Jin,[42] Y. Jin,[66] M. Q. Jing,[1,63] X. M. Jing,[63] T. Johansson,[75] S. Kabana,[33] N. Kalantar-Nayestanaki,[64] X. L. Kang,[9] X. S. Kang,[40] M. Kavatsyuk,[64] B. C. Ke,[80] V. Khachatryan,[27] A. Khoukaz,[68] R. Kiuchi,[1] O. B. Kolcu,[62a] B. Kopf,[3] M. Kuessner,[3] X. Kui,[1,63] N. Kumar,[26] A. Kupsc,[44,75] W. Kühn,[37] J. J. Lane,[67] P. Larin,[18] L. Lavezzi,[74a,74c] T. T. Lei,[71,58] Z. H. Lei,[71,58] M. Lellmann,[35] T. Lenz,[35] C. Li,[47] C. Li,[43] C. H. Li,[39] Cheng Li,[71,58] D. M. Li,[80] F. Li,[1,58] G. Li,[1] H. B. Li,[1,63] H. J. Li,[19] H. N. Li,[56,j] Hui Li,[43] J. R. Li,[61] J. S. Li,[59] Ke Li,[1] L. J. Li,[1,63] L. K. Li,[1] Lei Li,[48] M. H. Li,[43] P. R. Li,[38,l] Q. M. Li,[1,63] Q. X. Li,[50] R. Li,[17,31] S. X. Li,[12] T. Li,[50] W. D. Li,[1,63] W. G. Li,[1,a] X. Li,[1,63] X. H. Li,[71,58] X. L. Li,[50] X. Z. Li,[59] Xiaoyu Li,[1,63] Y. G. Li,[46,h] Z. J. Li,[59] Z. X. Li,[15] Z. Y. Li,[78] C. Liang,[42] H. Liang,[1,63] H. Liang,[71,58] Y. F. Liang,[54] Y. T. Liang,[31,63] G. R. Liao,[14] L. Z. Liao,[50] J. Libby,[26] A. Limphirat,[60] C. C. Lin,[55] D. X. Lin,[31,63] T. Lin,[1] B. J. Liu,[1] B. X. Liu,[76] C. Liu,[34] C. X. Liu,[1] F. H. Liu,[53] Fang Liu,[1] Feng Liu,[6] G. M. Liu,[56,j] H. Liu,[38,k,l] H. B. Liu,[15] H. M. Liu,[1,63] Huanhuan Liu,[1] Huihui Liu,[21] J. B. Liu,[71,58] J. Y. Liu,[1,63] K. Liu,[38,k,l] K. Y. Liu,[40] Ke Liu,[22] L. Liu,[71,58] L. C. Liu,[43] Lu Liu,[43] M. H. Liu,[12,g] P. L. Liu,[1] Q. Liu,[63] S. B. Liu,[71,58] T. Liu,[12,g] W. K. Liu,[43] W. M. Liu,[71,58] X. Liu,[38,k,l] X. Liu,[39] Y. Liu,[38,k,l] Y. Liu,[80] Y. B. Liu,[43] Z. A. Liu,[1,58,63] Z. D. Liu,[9] Z. Q. Liu,[50] X. C. Lou,[1,58,63] F. X. Lu,[59] H. J. Lu,[23] J. G. Lu,[1,58] X. L. Lu,[1] Y. Lu,[7] Y. P. Lu,[1,58] Z. H. Lu,[1,63] C. L. Luo,[41] J. R. Luo,[59] M. X. Luo,[79] T. Luo,[12,g] X. L. Luo,[1,58] X. R. Lyu,[63] Y. F. Lyu,[43] F. C. Ma,[40] H. Ma,[78] H. L. Ma,[1] J. L. Ma,[1,63] L. L. Ma,[50] M. M. Ma,[1,63] Q. M. Ma,[1] R. Q. Ma,[1,63] T. Ma,[71,58] X. T. Ma,[1,63] X. Y. Ma,[1,58] Y. Ma,[46,h] Y. M. Ma,[31] F. E. Maas,[18] M. Maggiora,[74a,74c] S. Malde,[69] Y. J. Mao,[46,h] Z. P. Mao,[1] S. Marcello,[74a,74c] Z. X. Meng,[66] J. G. Messchendorp,[13,64] G. Mezzadri,[29a] H. Miao,[1,63] T. J. Min,[42] R. E. Mitchell,[27]

X. H. Mo,[1,58,63] B. Moses,[27] N. Yu. Muchnoi,[4,c] J. Muskalla,[35] Y. Nefedov,[36] F. Nerling,[18,e] L. S. Nie,[20] I. B. Nikolaev,[4,c] Z. Ning,[1,58] S. Nisar,[11,m] Q. L. Niu,[38,k,l] W. D. Niu,[55] Y. Niu,[50] S. L. Olsen,[63] Q. Ouyang,[1,58,63] S. Pacetti,[28b,28c] X. Pan,[55] Y. Pan,[57] A. Pathak,[34] P. Patteri,[28a] Y. P. Pei,[71,58] M. Pelizaeus,[3] H. P. Peng,[71,58] Y. Y. Peng,[38,k,l] K. Peters,[13,e] J. L. Ping,[41] R. G. Ping,[1,63] S. Plura,[35] V. Prasad,[33] F. Z. Qi,[1] H. Qi,[71,58] H. R. Qi,[61] M. Qi,[42] T. Y. Qi,[12,g] S. Qian,[1,58] W. B. Qian,[63] C. F. Qiao,[63] X. K. Qiao,[80] J. J. Qin,[72] L. Q. Qin,[14] L. Y. Qin,[71,58] X. S. Qin,[50] Z. H. Qin,[1,58] J. F. Qiu,[1] Z. H. Qu,[72] C. F. Redmer,[35] K. J. Ren,[39] A. Rivetti,[74c] M. Rolo,[74c] G. Rong,[1,63] Ch. Rosner,[18] S. N. Ruan,[43] N. Salone,[44] A. Sarantsev,[36,d] Y. Schelhaas,[35] K. Schoenning,[75] M. Scodeggio,[29a] K. Y. Shan,[12,g] W. Shan,[24] X. Y. Shan,[71,58] Z. J. Shang,[38,k,l] J. F. Shangguan,[55] L. G. Shao,[1,63] M. Shao,[71,58] C. P. Shen,[12,g] H. F. Shen,[1,8] W. H. Shen,[63] X. Y. Shen,[1,63] B. A. Shi,[63] H. Shi,[71,58] H. C. Shi,[71,58] J. L. Shi,[12,g] J. Y. Shi,[1] Q. Q. Shi,[55] S. Y. Shi,[72] X. Shi,[1,58] J. J. Song,[19] T. Z. Song,[59] W. M. Song,[34,1] Y. J. Song,[12,g] Y. X. Song,[46,h,n] S. Sosio,[74a,74c] S. Spataro,[74a,74c] F. Stieler,[35] Y. J. Su,[63] G. B. Sun,[76] G. X. Sun,[1] H. Sun,[63] H. K. Sun,[1] J. F. Sun,[19] K. Sun,[61] L. Sun,[76] S. S. Sun,[1,63] T. Sun,[51,f] W. Y. Sun,[34] Y. Sun,[9] Y. J. Sun,[71,58] Y. Z. Sun,[1] Z. Q. Sun,[1,63] Z. T. Sun,[50] C. J. Tang,[54] G. Y. Tang,[1] J. Tang,[59] M. Tang,[71,58] Y. A. Tang,[76] L. Y. Tao,[72] Q. T. Tao,[25,i] M. Tat,[69] J. X. Teng,[71,58] V. Thoren,[75] W. H. Tian,[59] Y. Tian,[31,63] Z. F. Tian,[76] I. Uman,[62b] Y. Wan,[55] S. J. Wang,[50] B. Wang,[1] B. L. Wang,[63] Bo Wang,[71,58] D. Y. Wang,[46,h] F. Wang,[72] H. J. Wang,[38,k,l] J. J. Wang,[76] J. P. Wang,[50] K. Wang,[1,58] L. L. Wang,[1] M. Wang,[50] Meng Wang,[1,63] N. Y. Wang,[63] S. Wang,[12,g] S. Wang,[38,k,l] T. Wang,[12,g] T. J. Wang,[43] W. Wang,[59] W. Wang,[72] W. P. Wang,[35,71,o] X. Wang,[46,h] X. F. Wang,[38,k,l] X. J. Wang,[39] X. L. Wang,[12,g] X. N. Wang,[1] Y. Wang,[61] Y. D. Wang,[45] Y. F. Wang,[1,58,63] Y. L. Wang,[19] Y. N. Wang,[45] Y. Q. Wang,[1] Yaqian Wang,[17] Yi Wang,[61] Z. Wang,[1,58] Z. L. Wang,[72] Z. Y. Wang,[1,63] Ziyi Wang,[63] D. H. Wei,[14] F. Weidner,[68] S. P. Wen,[1] Y. R. Wen,[39] U. Wiedner,[3] G. Wilkinson,[69] M. Wolke,[75] L. Wollenberg,[3] C. Wu,[39] J. F. Wu,[1,8] L. H. Wu,[1] L. J. Wu,[1,63] X. Wu,[12,g] X. H. Wu,[34] Y. Wu,[71,58] Y. H. Wu,[55] Y. J. Wu,[31] Z. Wu,[1,58] L. Xia,[71,58] X. M. Xian,[39] B. H. Xiang,[1,63] T. Xiang,[46,h] D. Xiao,[38,k,l] G. Y. Xiao,[42] S. Y. Xiao,[1] Y. L. Xiao,[12,g] Z. J. Xiao,[41] C. Xie,[42] X. H. Xie,[46,h] Y. Xie,[50] Y. G. Xie,[1,58] Y. H. Xie,[6] Z. P. Xie,[71,58] T. Y. Xing,[1,63] C. F. Xu,[1,63] C. J. Xu,[59] G. F. Xu,[1] H. Y. Xu,[66] M. Xu,[71,58] Q. J. Xu,[16] Q. N. Xu,[30] W. Xu,[1] W. L. Xu,[66] X. P. Xu,[55] Y. C. Xu,[77] Z. P. Xu,[42] Z. S. Xu,[63] F. Yan,[12,g] L. Yan,[12,g] W. B. Yan,[71,58] W. C. Yan,[80] X. Q. Yan,[1] H. J. Yang,[51,f] H. L. Yang,[34] H. X. Yang,[1] Tao Yang,[1] Y. Yang,[12,g] Y. F. Yang,[43] Y. X. Yang,[1,63] Yifan Yang,[1,63] Z. W. Yang,[38,k,l] Z. P. Yao,[50] M. Ye,[1,58] M. H. Ye,[8] J. H. Yin,[1] Z. Y. You,[59] B. X. Yu,[1,58,63] C. X. Yu,[43] G. Yu,[1,63] J. S. Yu,[25,i] T. Yu,[72] X. D. Yu,[46,h] Y. C. Yu,[80] C. Z. Yuan,[1,63] J. Yuan,[34] L. Yuan,[2] S. C. Yuan,[1] Y. Yuan,[1,63] Y. J. Yuan,[45] Z. Y. Yuan,[59] C. X. Yue,[39] A. A. Zafar,[73] F. R. Zeng,[50] S. H. Zeng,[72] X. Zeng,[12,g] Y. Zeng,[25,i] Y. J. Zeng,[59] X. Y. Zhai,[34] Y. C. Zhai,[50] Y. H. Zhan,[59] A. Q. Zhang,[1,63] B. L. Zhang,[1,63] B. X. Zhang,[1] D. H. Zhang,[43] G. Y. Zhang,[19] H. Zhang,[71,58] H. Zhang,[80] H. C. Zhang,[1,58,63] H. H. Zhang,[59] H. H. Zhang,[34] H. Q. Zhang,[1,58,63] H. R. Zhang,[71,58] H. Y. Zhang,[1,58] J. Zhang,[59] J. Zhang,[80] J. J. Zhang,[52] J. L. Zhang,[20] J. Q. Zhang,[41] J. S. Zhang,[12,g] J. W. Zhang,[1,58,63] J. X. Zhang,[38,k,l] J. Y. Zhang,[1] J. Z. Zhang,[1,63] Jianyu Zhang,[63] L. M. Zhang,[61] Lei Zhang,[42] P. Zhang,[1,63] Q. Y. Zhang,[34] R. Y. Zhang,[38,k,l] Shuihan Zhang,[1,63] Shulei Zhang,[25,i] X. D. Zhang,[45] X. M. Zhang,[1] X. Y. Zhang,[50] Y. Zhang,[72] Y. T. Zhang,[80] Y. H. Zhang,[1,58] Y. M. Zhang,[39] Yan Zhang,[71,58] Yao Zhang,[1] Z. D. Zhang,[1] Z. H. Zhang,[1] Z. L. Zhang,[34] Z. Y. Zhang,[43] Z. Y. Zhang,[76] Z. Z. Zhang,[45] G. Zhao,[1] J. Y. Zhao,[1,63] J. Z. Zhao,[1,58] Lei Zhao,[71,58] Ling Zhao,[1] M. G. Zhao,[43] N. Zhao,[78] R. P. Zhao,[63] S. J. Zhao,[80] Y. B. Zhao,[1,58] Y. X. Zhao,[31,63] Z. G. Zhao,[71,58] A. Zhemchugov,[36,b] B. Zheng,[72] B. M. Zheng,[34] J. P. Zheng,[1,58] W. J. Zheng,[1,63] Y. H. Zheng,[63] B. Zhong,[41] X. Zhong,[59] H. Zhou,[50] J. Y. Zhou,[34] L. P. Zhou,[1,63] S. Zhou,[6] X. Zhou,[76] X. K. Zhou,[6] X. R. Zhou,[71,58] X. Y. Zhou,[39] Y. Z. Zhou,[12,g] J. Zhu,[43] K. Zhu,[1] K. J. Zhu,[1,58,63] K. S. Zhu,[12,g] L. Zhu,[34] L. X. Zhu,[63] S. H. Zhu,[70] S. Q. Zhu,[42] T. J. Zhu,[12,g] W. D. Zhu,[41] Y. C. Zhu,[71,58] Z. A. Zhu,[1,63] J. H. Zou,[1] and J. Zu[71,58]

(BESIII Collaboration)

[1]*Institute of High Energy Physics, Beijing 100049, People's Republic of China*
[2]*Beihang University, Beijing 100191, People's Republic of China*
[3]*Bochum Ruhr-University, D-44780 Bochum, Germany*
[4]*Budker Institute of Nuclear Physics SB RAS (BINP), Novosibirsk 630090, Russia*
[5]*Carnegie Mellon University, Pittsburgh, Pennsylvania 15213, USA*
[6]*Central China Normal University, Wuhan 430079, People's Republic of China*
[7]*Central South University, Changsha 410083, People's Republic of China*
[8]*China Center of Advanced Science and Technology, Beijing 100190, People's Republic of China*
[9]*China University of Geosciences, Wuhan 430074, People's Republic of China*
[10]*Chung-Ang University, Seoul, 06974, Republic of Korea*

[11]COMSATS University Islamabad, Lahore Campus, Defence Road, Off Raiwind Road, 54000 Lahore, Pakistan
[12]Fudan University, Shanghai 200433, People's Republic of China
[13]GSI Helmholtzcentre for Heavy Ion Research GmbH, D-64291 Darmstadt, Germany
[14]Guangxi Normal University, Guilin 541004, People's Republic of China
[15]Guangxi University, Nanning 530004, People's Republic of China
[16]Hangzhou Normal University, Hangzhou 310036, People's Republic of China
[17]Hebei University, Baoding 071002, People's Republic of China
[18]Helmholtz Institute Mainz, Staudinger Weg 18, D-55099 Mainz, Germany
[19]Henan Normal University, Xinxiang 453007, People's Republic of China
[20]Henan University, Kaifeng 475004, People's Republic of China
[21]Henan University of Science and Technology, Luoyang 471003, People's Republic of China
[22]Henan University of Technology, Zhengzhou 450001, People's Republic of China
[23]Huangshan College, Huangshan 245000, People's Republic of China
[24]Hunan Normal University, Changsha 410081, People's Republic of China
[25]Hunan University, Changsha 410082, People's Republic of China
[26]Indian Institute of Technology Madras, Chennai 600036, India
[27]Indiana University, Bloomington, Indiana 47405, USA
[28a]INFN Laboratori Nazionali di Frascati, I-00044, Frascati, Italy
[28b]INFN Sezione di Perugia, I-06100, Perugia, Italy
[28c]University of Perugia, I-06100, Perugia, Italy
[29a]INFN Sezione di Ferrara, I-44122, Ferrara, Italy
[29b]University of Ferrara, I-44122, Ferrara, Italy
[30]Inner Mongolia University, Hohhot 010021, People's Republic of China
[31]Institute of Modern Physics, Lanzhou 730000, People's Republic of China
[32]Institute of Physics and Technology, Peace Avenue 54B, Ulaanbaatar 13330, Mongolia
[33]Instituto de Alta Investigación, Universidad de Tarapacá, Casilla 7D, Arica 1000000, Chile
[34]Jilin University, Changchun 130012, People's Republic of China
[35]Johannes Gutenberg University of Mainz, Johann-Joachim-Becher-Weg 45, D-55099 Mainz, Germany
[36]Joint Institute for Nuclear Research, 141980 Dubna, Moscow region, Russia
[37]Justus-Liebig-Universitaet Giessen, II. Physikalisches Institut, Heinrich-Buff-Ring 16, D-35392 Giessen, Germany
[38]Lanzhou University, Lanzhou 730000, People's Republic of China
[39]Liaoning Normal University, Dalian 116029, People's Republic of China
[40]Liaoning University, Shenyang 110036, People's Republic of China
[41]Nanjing Normal University, Nanjing 210023, People's Republic of China
[42]Nanjing University, Nanjing 210093, People's Republic of China
[43]Nankai University, Tianjin 300071, People's Republic of China
[44]National Centre for Nuclear Research, Warsaw 02-093, Poland
[45]North China Electric Power University, Beijing 102206, People's Republic of China
[46]Peking University, Beijing 100871, People's Republic of China
[47]Qufu Normal University, Qufu 273165, People's Republic of China
[48]Renmin University of China, Beijing 100872, People's Republic of China
[49]Shandong Normal University, Jinan 250014, People's Republic of China
[50]Shandong University, Jinan 250100, People's Republic of China
[51]Shanghai Jiao Tong University, Shanghai 200240, People's Republic of China
[52]Shanxi Normal University, Linfen 041004, People's Republic of China
[53]Shanxi University, Taiyuan 030006, People's Republic of China
[54]Sichuan University, Chengdu 610064, People's Republic of China
[55]Soochow University, Suzhou 215006, People's Republic of China
[56]South China Normal University, Guangzhou 510006, People's Republic of China
[57]Southeast University, Nanjing 211100, People's Republic of China
[58]State Key Laboratory of Particle Detection and Electronics, Beijing 100049, Hefei 230026, People's Republic of China
[59]Sun Yat-Sen University, Guangzhou 510275, People's Republic of China
[60]Suranaree University of Technology, University Avenue 111, Nakhon Ratchasima 30000, Thailand
[61]Tsinghua University, Beijing 100084, People's Republic of China
[62a]Turkish Accelerator Center Particle Factory Group, Istinye University, 34010, Istanbul, Turkey
[62b]Near East University, Nicosia, North Cyprus, 99138, Mersin 10, Turkey
[63]University of Chinese Academy of Sciences, Beijing 100049, People's Republic of China

[64]*University of Groningen, NL-9747 AA Groningen, The Netherlands*
[65]*University of Hawaii, Honolulu, Hawaii 96822, USA*
[66]*University of Jinan, Jinan 250022, People's Republic of China*
[67]*University of Manchester, Oxford Road, Manchester, M13 9PL, United Kingdom*
[68]*University of Muenster, Wilhelm-Klemm-Strasse 9, 48149 Muenster, Germany*
[69]*University of Oxford, Keble Road, Oxford OX13RH, United Kingdom*
[70]*University of Science and Technology Liaoning, Anshan 114051, People's Republic of China*
[71]*University of Science and Technology of China, Hefei 230026, People's Republic of China*
[72]*University of South China, Hengyang 421001, People's Republic of China*
[73]*University of the Punjab, Lahore-54590, Pakistan*
[74a]*University of Turin and INFN, I-10125, Turin, Italy*
[74b]*University of Eastern Piedmont, I-15121, Alessandria, Italy*
[74c]*INFN, I-10125, Turin, Italy*
[75]*Uppsala University, Box 516, SE-75120 Uppsala, Sweden*
[76]*Wuhan University, Wuhan 430072, People's Republic of China*
[77]*Yantai University, Yantai 264005, People's Republic of China*
[78]*Yunnan University, Kunming 650500, People's Republic of China*
[79]*Zhejiang University, Hangzhou 310027, People's Republic of China*
[80]*Zhengzhou University, Zhengzhou 450001, People's Republic of China*

[a]Deceased.
[b]Also at the Moscow Institute of Physics and Technology, Moscow 141700, Russia.
[c]Also at the Novosibirsk State University, Novosibirsk 630090, Russia.
[d]Also at the NRC "Kurchatov Institute", PNPI, 188300 Gatchina, Russia.
[e]Also at Goethe University Frankfurt, 60323 Frankfurt am Main, Germany.
[f]Also at Key Laboratory for Particle Physics, Astrophysics and Cosmology, Ministry of Education; Shanghai Key Laboratory for Particle Physics and Cosmology; Institute of Nuclear and Particle Physics, Shanghai 200240, People's Republic of China.
[g]Also at Key Laboratory of Nuclear Physics and Ion-beam Application (MOE) and Institute of Modern Physics, Fudan University, Shanghai 200443, People's Republic of China.
[h]Also at State Key Laboratory of Nuclear Physics and Technology, Peking University, Beijing 100871, People's Republic of China.
[i]Also at School of Physics and Electronics, Hunan University, Changsha 410082, China.
[j]Also at Guangdong Provincial Key Laboratory of Nuclear Science, Institute of Quantum Matter, South China Normal University, Guangzhou 510006, China.
[k]Also at MOE Frontiers Science Center for Rare Isotopes, Lanzhou University, Lanzhou 730000, People's Republic of China.
[l]Also at Lanzhou Center for Theoretical Physics, Lanzhou University, Lanzhou 730000, People's Republic of China.
[m]Also at the Department of Mathematical Sciences, IBA, Karachi 75270, Pakistan.
[n]Also at Ecole Polytechnique Federale de Lausanne (EPFL), CH-1015 Lausanne, Switzerland.
[o]Also at Helmholtz Institute Mainz, Staudinger Weg 18, D-55099 Mainz, Germany.